

Salt Fusion: An Approach to Improve Pore Interconnectivity within Tissue Engineering Scaffolds

WILLIAM L. MURPHY, M.S.,¹ ROBERT G. DENNIS, Ph.D.,^{1,2,5}
JOEL L. KILENY, B.S.,¹ and DAVID J. MOONEY, Ph.D.^{1,3,4}

ABSTRACT

Macroporous scaffolds composed of biodegradable polymers have found extensive use as three-dimensional substrates either for *in vitro* cell seeding followed by transplantation, or as conductive substrates for direct implantation *in vivo*. Methods abound for creation of macroporous scaffolds for tissue engineering, and common methods typically employ a solid porogen within a three-dimensional polymer matrix to create a well-defined pore size, pore structure, and total scaffold porosity. This study describes an approach to impart improved pore interconnectivity to polymer scaffolds for tissue engineering by partially fusing the solid porogen together prior to creation of a continuous polymer matrix. Three dimensional, porous scaffolds of the copolymer 85:15 poly(lactide-co-glycolide) were fabricated via either a solvent casting/particulate leaching process, or a gas foaming/particulate leaching process. Prior to creation of a continuous polymer matrix the NaCl crystals, which serve as the solid porogen, are partially fused via treatment in 95% humidity. Scanning electron micrographs clearly display fused salt crystals and an enhancement in pore interconnectivity in the salt fused scaffolds prepared via both solvent casting and gas foaming, and the extent of pore interconnectivity is enhanced with longer treatment times. Fusion of salt crystal for 24 h increased the radius of curvature of salt crystals, and led to a twofold increase in the compressive modulus of solvent cast scaffolds (total porosity of $97 \pm 1\%$). Fusion of NaCl crystals prior to gas foaming resulted in a decrease in scaffold compressive modulus from $277 \pm 60\text{k Pa}$ to $187 \pm 30\text{k Pa}$ (total porosity of $94 \pm 1\%$). The resulting highly interconnected scaffolds have implications for facilitated cell migration, abundant cell-cell interaction, and potentially improved neural and vascular growth within tissue engineering scaffolds.

INTRODUCTION

POROUS SCAFFOLDS composed of biodegradable polymers have found extensive use in the engineering of several tissue types.^{1,2} Various tissue engineering strategies employ scaffolding materials as three-dimensional substrates either for *in vitro* cell seeding followed by transplantation (cell-based approaches), or as conductive substrates for direct implantation *in vivo* (conductive approaches).³ The degree of success of

The ¹Department of Biomedical Engineering, ²Institute of Gerontology, ³Department of Biologic and Materials Sciences, and ⁴Department of Chemical Engineering, University of Michigan, Ann Arbor, Michigan.

⁵Artificial Intelligence Laboratory, MIT, Cambridge, Massachusetts.

these schemes depends, in part, on the internal structure of the scaffold system. Numerous applications require a highly interconnected, macroporous structure within a scaffold system to encourage neural and fibrovascular ingrowth, promote uniformity of *in vitro* cell seeding, and facilitate migration of both seeded cells and cells migrating from a contiguous *in vivo* site. Besides being crucial in nervous system applications, neural tissue ingrowth may be critically important in other tissues requiring sensory control, such as functional skeletal muscle, cardiac, and renal tissues. Fibrovascular ingrowth promotes mass transport to and from a developing tissue, and is particularly vital for the engineering of bulk tissues (i.e., bone, liver, skeletal muscle) in which cells do not have an avenue for procurement of oxygen and nutrients and excretion of metabolic waste. Furthermore, uniform cell seeding and facile cell migration are important to promote homogeneity of the developing tissue in both conductive and cell-based tissue engineering approaches.

Commonly used methods for processing biodegradable polymers in tissue engineering applications involve three steps: (1) inclusion of a dispersed porogen within a discontinuous polymer matrix; (2) a technique leading to the creation of a continuous polymer matrix around the dispersed porogen; and (3) leaching of the porogen from the polymer matrix leaving a macroporous, biodegradable polymer scaffold.⁴ Although other techniques have been used to create a continuous polymer matrix in step 2 above,⁴ this study will focus on the solvent casting⁵ and gas foaming⁶ processes in particular due to their frequent use to engineer numerous tissue types.⁷⁻¹¹ In the solvent casting process,⁵ a polymer is dissolved in a suitable solvent and added to a porogen-containing mold, and then the porogen is dispersed. The solvent is then allowed to evaporate from the mixture under ambient conditions leaving a polymer matrix containing a porogen which can then be leached out in an appropriate solvent (usually H₂O). In the gas foaming process⁶ polymer particles are mixed with porogen particles and the mixture is compressed into a solid mixture of a discontinuous polymer with an interspersed porogen. The resulting pellet is then exposed to high pressure CO₂ gas, and after the pressure is allowed to equilibrate over a period of time the pressure is rapidly released causing a thermodynamic instability in the polymer component of the mixture. The instability causes the polymer to foam, and the originally discontinuous polymer particles fuse together to form a continuous polymer matrix around interspersed porogen particles, which are then leached out in a solvent. In each of these processes the degree of interconnection between pores in the resulting scaffold is determined by the interconnection of porogen particles during the solvent evaporation or polymer foaming steps, respectively. Because the porogen is dispersed, the degree of interconnection between porogen particles is not actively controlled, and thus the interconnectivity of pores in the final scaffold product is uncontrolled. Enhancement in and control over porogen interconnectivity may be an important concern in various tissue engineering strategies in view of the substantial advantages of pore interconnectivity within scaffolds.

This study was undertaken to develop a process for producing macroporous, biodegradable tissue engineering scaffolds with improved pore interconnectivity. Specifically, the goal was to vary existing processing methods for biodegradable polymers to designedly connect pores, while controlling the extent of pore interconnection. Pores are connected via the fusion of a salt porogen prior to formation of a three-dimensional polymer scaffold. Thus, after formation of the three-dimensional scaffold, removal of the fused porogen matrix leaves a highly interconnected pore structure. The copolymer poly(lactide-co-glycolide) (PLG) was specifically chosen for this study due to its biocompatibility, controllable biodegradability into natural metabolites, and widespread previous use as a macroporous tissue engineering scaffold system.^{7-11,14,15} Improvement in pore interconnectivity may result in a more effective utilization of porous biodegradable scaffolds in various tissue engineering strategies, particularly in muscular and neural applications.

MATERIALS AND METHODS

Sample preparation

Poly(lactide-co-glycolide) pellets with a lactide/glycolide ratio of 85:15 were obtained from Medisorb, Inc. (IV = 0.78 dL/g) and Boehringer-Ingelheim Inc. (IV = 1.5 dL/g). Higher inherent viscosity PLG was used in the solvent casting process to ensure that the scaffolds would retain adequate mechanical integrity despite their relatively high porosity (~97%). Porous scaffolds were prepared either by solvent casting/par-

ticulate leaching, or gas foaming/particulate leaching processes using NaCl as the particulate porogen. The solvent cast scaffolds were prepared as described elsewhere⁵ with two major differences: (1) NaCl molds were not dispersed within the polymer solution prior to solvent evaporation (the polymer solution was poured into a NaCl-containing mold with no dispersion); and (2) the resulting NaCl molds were subjected to 95% humidity for periods from 0 to 24 h to achieve fusion of NaCl crystals prior to solvent casting. The gas foamed scaffolds were also prepared as described elsewhere⁶ except that the compression molded NaCl/polymer solid pellets were subjected to 95% humidity for periods of 0–24 h to achieve salt fusion prior to polymer foaming. Following treatment in 95% humidity, samples were dried in a vacuum desiccator for 48 h before further processing. A closed, water-jacketed cell culture incubator (Forma Scientific, Inc.) held at 37°C was used to create a 95% humidity environment for fusion of NaCl crystals.

Scaffolds were circular disks with a diameter of 12 mm and a thickness of 3 mm. The pore size range was controlled by using NaCl particles with a diameter of 250–425 μm in the processing. The total porosity of scaffolds was calculated using the known density of the solid polymer, the measured polymer mass of the scaffold, and the measured external volume of the scaffold.

Materials characterization

Electron microscopy. Fused salt molds were bisected and imaged prior to solvent casting to observe the extent of NaCl crystal fusion. In addition, polymer scaffolds were bisected after preparation via freeze fracture. A carbon coating was evaporated onto the surface of each bisected salt mold and polymer scaffold, and samples were imaged under high vacuum using a Hitachi S-3200N SEM operating at 20–30 kV.

Measurement of moduli. Compressive moduli of scaffolds were determined using an MTS Bionix 100 mechanical testing system. Samples were compressed between platens with a constant deformation rate of 1 mm/min. Compression plates had a diameter of 45 mm and thus covered the entire 12-mm diameter surface of the scaffold. A small preload was applied to each sample to ensure that the entire scaffold surface was in contact with the compression plates prior to testing, and the distance between plates prior to each test was equal to the measured thickness of the scaffold being tested. Compressive moduli were determined for scaffolds without salt fusion and for each of four samples for each salt fusion time. At each time point, experimental moduli were compared to control moduli via a Student's *t* test to reveal significant differences in compressive modulus.

Image analysis. The radius of curvature of salt crystals was calculated from electron micrographs using microsoft paint software. The pixel size for each image was calibrated, and the pencil tool was used to mark tangent points on crystal edges. The calibration values and pixel coordinates were then used to calculate the cord length between tangent points, which was multiplied by $\sqrt{2}/2$ to obtain the crystal radius of curvature. The diameter of holes in pore walls was determined by measuring the major and minor diametral axes of each hole using microsoft paint and taking the average.

Statistical analysis. Four scaffolds were prepared, treated, and analyzed for NaCl incubation times from 0 to 24 h. Values on graphs represent means and standard deviations. Statistical analysis was performed using InStat software, version 2.01.

RESULTS

Incubation of NaCl crystals in 95% humidity resulted in fusion of the crystals, creating a highly interconnected NaCl matrix (Fig. 1a,b). Fusion of salt crystals prior to addition of PLG in chloroform (solvent casting) resulted in enhanced pore interconnectivity within the scaffold. The pore structure within the scaffolds (Fig. 2) appears similar to the structure of the fused salt matrix (Fig. 1a,b), as expected. Pores within the cross-section of 1 h salt fusion (SF) samples display a defined pore structure with intermittent holes in pore walls (Fig. 2a,c), while the cross-section of scaffolds created from 24-h SF samples display a much

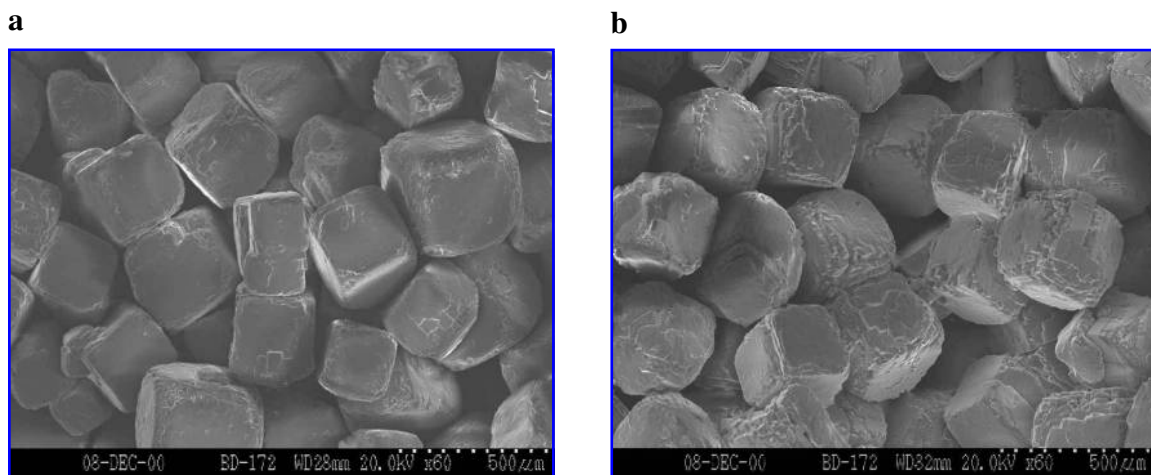


FIG. 1. Electron micrographs of the cross-section of a NaCl matrix of salt crystals fused via (a) 12-h or (b) 24-h treatment in 95% humidity.

less organized pore structure and a very large density of holes in pore walls (Fig. 2b,d). The hole size increased significantly with fusion time, from an average diameter of $31 \pm 10 \mu\text{m}$ after 1 h of fusion to $78 \pm 21 \mu\text{m}$ after 24 h of fusion ($p < 0.05$). In addition, the pore walls in the 24-h SF scaffolds display thickness contours such that the walls appear thicker in the area adjacent to the holes in pore walls and along the outer diameter of the walls (Fig. 2d). A higher magnification view of a pore wall within a 24-hr SF scaffold further displays the contoured structure of the pore walls (Fig. 2e). The salt fusion process had no effect on the porosity of the scaffolds, and the calculated total porosities of the solvent cast scaffolds for each salt fusion time period were $97 \pm 1\%$.

A close examination of the electron micrographs of the solvent cast scaffolds formed after 1 and 24 h of NaCl fusion indicate that the exposure to 95% humidity has caused several important changes in the structure of the salt grains. In addition to the formation of bridges between grains at the points of contact, the radius of curvature of edges and corners in individual grains of salt has increased (Fig. 1a,b). These changes are shown schematically (Fig. 3). The increased radius of curvature at the edges and corners of each grain of salt results in an increased sphericity of each grain (Fig. 4) and thus in each resulting pore in the scaffold. The mean radius of curvature of the crystal edges increased from $19 \pm 10 \mu\text{m}$ to $32 \pm 15 \mu\text{m}$ after 12 h of exposure to 95% humidity, then to $62 \pm 18 \mu\text{m}$ after a full 24 h of exposure (Fig. 4). As a result, many of the smaller crystals became nearly spherical in shape after 24 h of fusion. One additional consequence is that thicker polymeric struts may be formed in the space vacated by the corners and edges of each salt crystal, which may result in the thickness contours in pore walls described above and in varied mechanical properties.

Fusion of salt crystals in PLG/NaCl pellets prior to gas foaming also resulted in a pronounced variation in pore structure. The cross-section of 1-h SF samples (Fig. 5a,c) shows small holes in pore walls similar to those in the solvent cast 1-h SF samples. The 24-hr salt fusion samples lack a defined pore structure and pores appear to simply feed into each other (Fig. 5b,d). The gas foamed SF scaffolds do not display any of the contours in pore walls observed in the solvent cast SF samples. Again, the salt fusion process had no effect on the total scaffold porosity. The total porosities of the gas foamed scaffolds for each salt fusion time period were $94 \pm 1\%$.

Fusion of salt crystals for 24 h resulted in a twofold increase in the compressive modulus of the solvent cast scaffolds (Fig. 6a). No significant modulus change is observed after 1 or 12 h of salt fusion. Alternatively, there was a statistically significant decrease in the compressive modulus of gas foamed scaffolds processed using salt fusion when compared with control scaffolds (Fig. 6b).

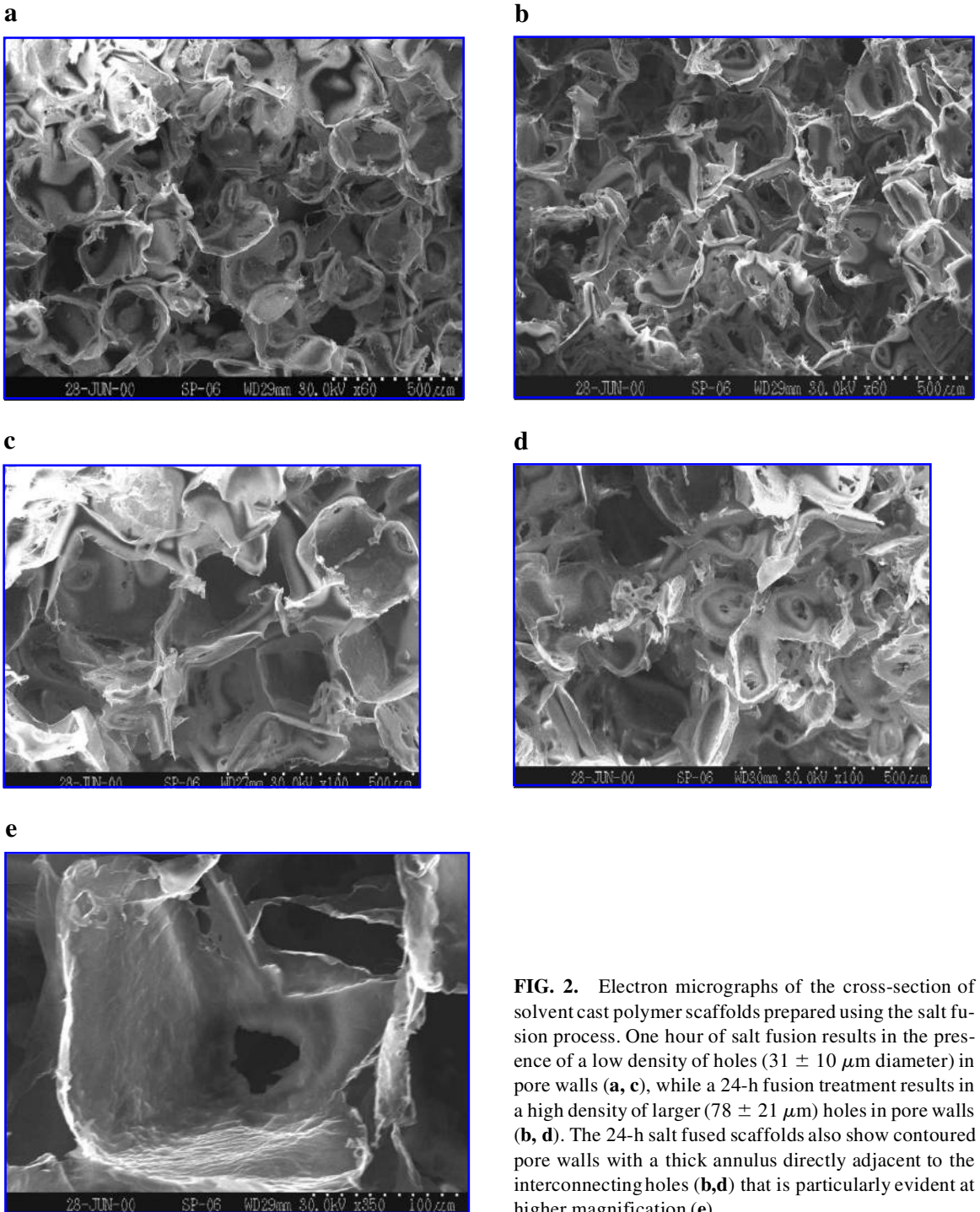


FIG. 2. Electron micrographs of the cross-section of solvent cast polymer scaffolds prepared using the salt fusion process. One hour of salt fusion results in the presence of a low density of holes ($31 \pm 10 \mu\text{m}$ diameter) in pore walls (**a, c**), while a 24-h fusion treatment results in a high density of larger ($78 \pm 21 \mu\text{m}$) holes in pore walls (**b, d**). The 24-h salt fused scaffolds also show contoured pore walls with a thick annulus directly adjacent to the interconnecting holes (**b,d**) that is particularly evident at higher magnification (**e**).

DISCUSSION

NaCl crystals can be fused via exposure to a solvent-rich environment (95% humidity), resulting in enhanced pore interconnectivity within both solvent cast and gas foamed PLG scaffolds. Fusion of a NaCl matrix prior to solvent casting results in formation of holes in pore walls, and the diameter and sphericity

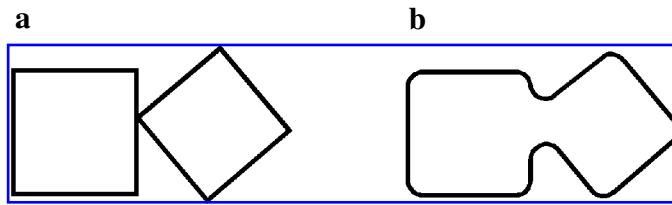


FIG. 3. Salt fusion process by solid diffusion in a solvent-enriched (95% humidity) atmosphere. **(a)** Prior to fusion, the salt grains have small areas of contact and sharp radii at edges and corners. **(b)** After 24 h of exposure to 95% humidity, diffusion near the contact points has resulted in the formation of thick salt bridges between particles, as well as an increase in the radius of curvature at the edges and corners of each salt particle.

of these holes increases with increasing salt fusion treatment. Salt fusion treatment causes an increase in the compressive modulus of solvent cast scaffolds, possibly due to the formation of thick annular struts adjacent to holes in pore walls. Enhanced pore interconnectivity may be useful in a variety of tissue engineering applications, particularly those requiring intimate cell–cell contact (i.e., neural and muscular applications). Also, because the salt fusion method imparts improved pore interconnectivity in both the solvent casting and gas foaming processes, the concept may be applicable to other solid porogen-based methods for producing macro- or micro-porous material systems with high interconnectivity.

Utilization of a fused NaCl mold (Fig. 1a,b) in a solvent casting, particulate leaching method resulted in the formation of holes between pore walls in the scaffold (Fig. 2a–e). With increased salt fusion time the pore structure within the scaffold cross sections became less organized (Fig. 2b,d). The apparent lack of an organized pore structure is likely due to the excellent interconnectivity of the salt fused samples, which reduces the presence of well-organized, largely closed-off pores. Upon scaffold bisection many of the pores have flattened out due to their lack of a continuous pore wall. In effect, the increased continuity of the fused salt matrix creates corresponding discontinuity in the polymer matrix, leading to large openings between pores and superior interconnectivity. Additionally, intact samples could not be fabricated using salt fusion time periods of 48 h or more. This further supports the inverse relationship between salt matrix continuity and polymer scaffold continuity. Previous studies using solvent casting, particulate leaching processes in which salt is dispersed allow no control over pore interconnectivity in accord with the holes in pore walls displayed in the present study.^{5,7,12} In a recent study, investigators utilized heat to fuse polymeric porogen

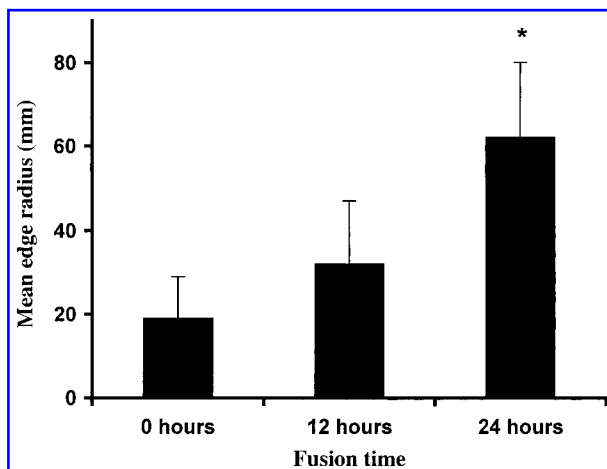


FIG. 4. Increase in the radius of curvature of salt crystal edges prior to addition of polymer in the solvent casting/particulate leaching method. Radii were measured from electron micrographs of salt crystals fused for 0, 12, and 24 h. Based on an ANOVA followed by comparisons between group means (Bonferroni *t* tests), the change in mean edge radius from 0 to 12 h was not significant ($p > 0.05$); however, the change from 12 h to 24 h was extremely significant ($p < 0.001$).

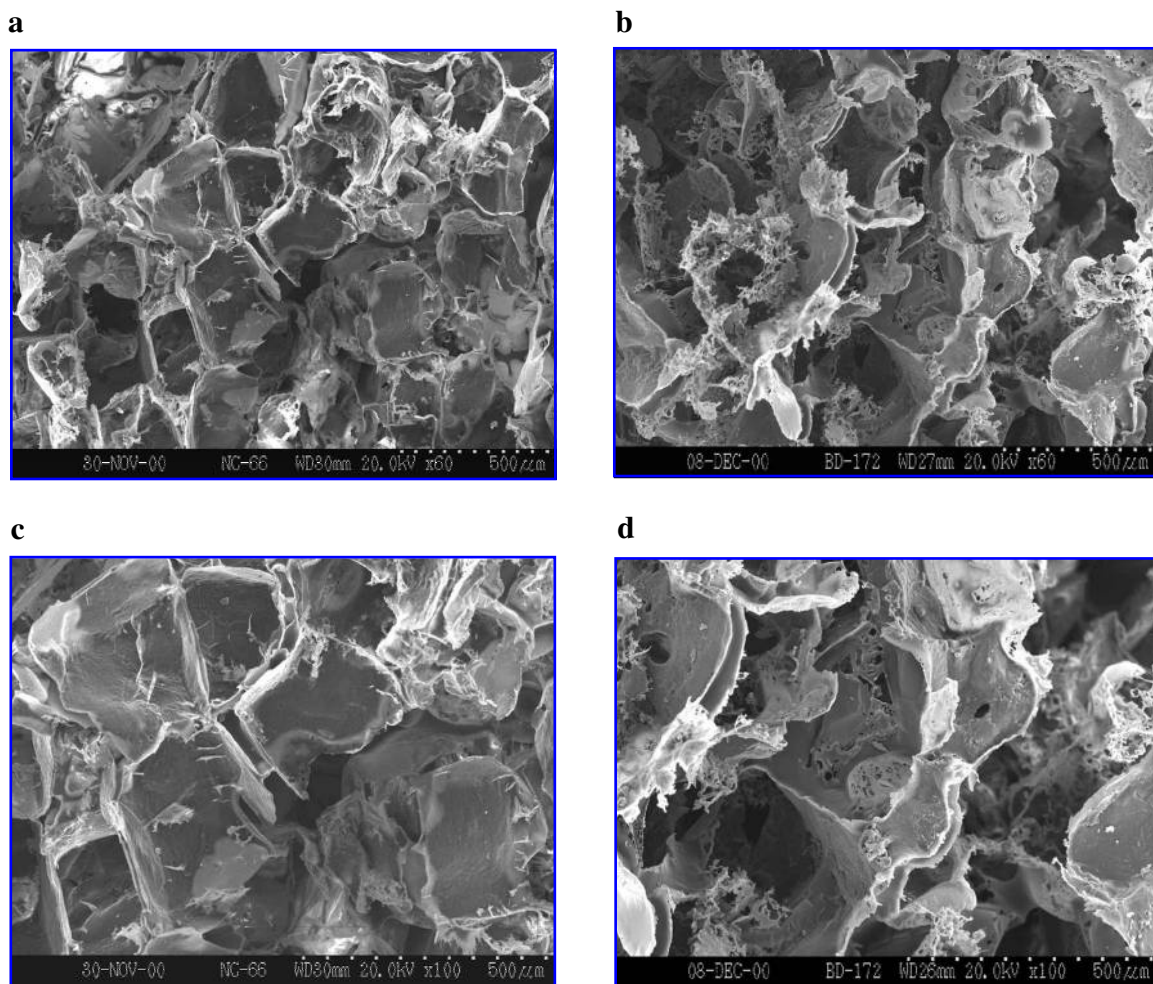


FIG. 5. Electron micrographs of the cross-section of gas foamed polymer scaffolds prepared using the salt fusion process. One hour of salt fusion results in the presence of a few very small holes in pore walls (**a,c**) similar to those in the solvent cast scaffolds. The 24-h salt fused scaffolds display a disorganized pore structure in which adjacent pores seem to feed into each other (**b,d**).

particles together prior to solvent casting.¹³ Although the use of heat may prove useful in several tissue engineering applications, the localized dissolution approach described herein may hold more broad applicability due to its potential for room temperature fusion of several types of porogen particle (both organic and inorganic), and its potential addition to processing techniques that can include bioactive inductive factors (i.e., gas foaming/particulate leaching).

The fusion of NaCl crystals within PLG/NaCl mixtures prior to gas foaming also has a pronounced effect on pore structure. The pores within the 24-h SF gas foamed scaffolds appear to feed directly into one another, implying a very high interconnectivity without a large decrease in scaffold compressive moduli (Fig. 6b). The gas foaming process has previously been used to process scaffolds containing biologically active vascular endothelial growth factor^{14,15} and plasmid DNA encoding for platelet-derived growth factor¹⁶ to promote ingrowth of vascular tissue. Adding the salt fusion method reported herein to previous studies geared towards promotion of rapid angiogenesis may lead to the formation of a highly interconnected vascular supply throughout the interior of a tissue engineering scaffold. Achieving vascular ingrowth to maximum depths within a scaffold system is a substantial goal in bulk tissue engineering strategies, and a highly interconnected pore structure may be advantageous for optimal vascular tissue ingrowth.

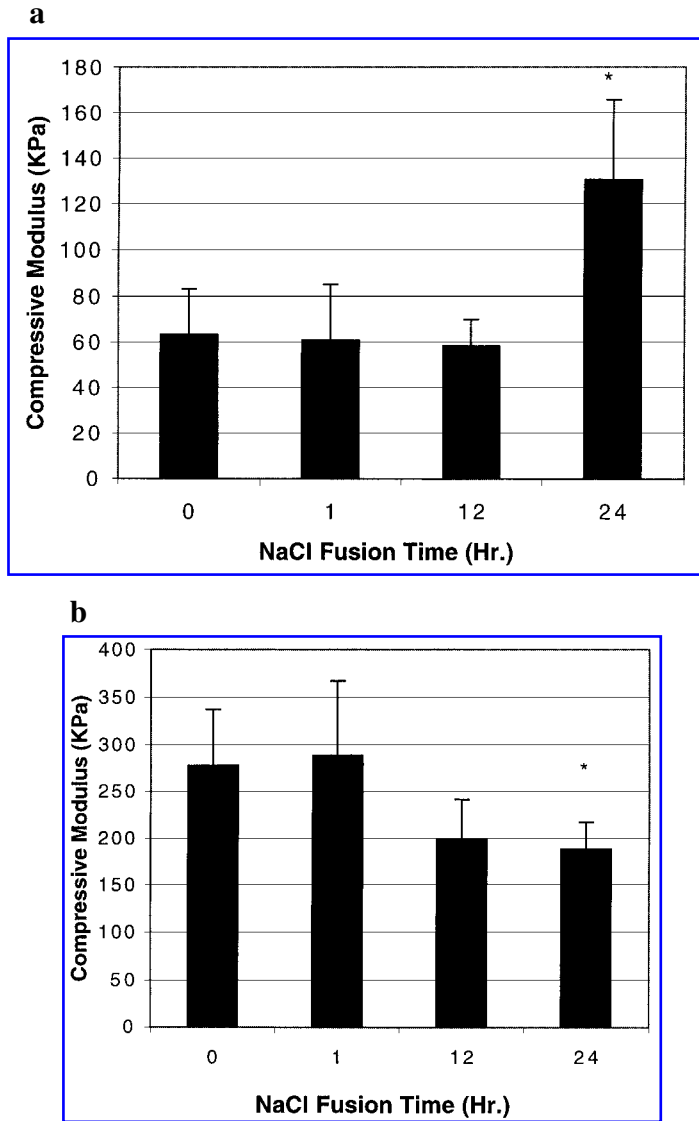


FIG. 6. Compressive modulus of scaffolds subjected to salt fusion for various periods of time, and prepared via either solvent casting (**a**) or gas foaming (**b**). Values represent mean and standard deviation ($n = 4$), and * indicates statistical significance relative to control ($p < 0.05$).

When exposed to humid environments, adjacent salt crystals fuse in a process called “caking,” which often results in the formation of large agglomerations of rock salt or improperly stored table salt. Anticaking agents, such as calcium silicate, are added to table salt to prevent caking, essentially by absorbing moisture inside the package that otherwise would be absorbed into the surface of the salt grains. The rate of diffusion of atoms within the solid salt crystal lattice is increased by the presence of absorbed water. The increased diffusion allows the surfaces of the contacting salt particles to coalesce, forming bridges between particles in a process similar to that used for solid sintering of non-vitreous ceramic materials. The individual particles begin to coalesce because, in the process, the total surface area of the salt particles is reduced, thus reducing the surface energy.¹⁷ The increased sphericity of each grain of salt (Fig. 4) is also thermodynamically favored, since this also reduces the total surface energy of each particle.

The solvent cast scaffolds had a significantly increased compressive modulus after 24 h of salt fusion (Fig. 6a), whereas the gas foamed scaffolds did not (Fig. 6b). We hypothesize that, for the solvent cast scaffold,

fold, the thicker struts of PLG material that were permitted to form in the space vacated by rounded corners and edges of the salt particles formed a stiffer structure, without an increase in the volume fraction of PLG in the scaffold. A similar increase in the modulus of the gas foamed scaffolds did not occur with increased NaCl fusion time. This may be due to the presence of PLG particles during the salt fusion in the gas foaming process. Undoubtedly there is some void space for interaction between adjacent NaCl crystals, even in the presence of both types of particles (NaCl and PLG). We hypothesize that the displacement of the salt surface resulting from diffusion was restricted to movement within the available void space. Evidence in support of this is clear in Figure 5b,d, in which the scaffold is composed of microperforated sheets, not present in the solvent cast scaffold, suggesting that during the NaCl fusion process the moving salt crystal surface was obstructed by, and perhaps flowed around, the smaller PLG particles. Thus, although bridges were formed between adjacent salt particles, the movement of the crystal surfaces was constrained by the presence of the PLG particles. This may have prevented the growth of void spaces in the salt structure that would lead to the formation of thick-section struts in the PLG scaffold, explaining why there was increased pore interconnectivity, but not increased compressive modulus, in the gas foamed scaffolds.

The salt fusion method described herein may be most applicable to the engineering of neural and muscular tissues due to their dependence on pore interconnectivity. Regenerative processes in the bridging of neural tissue defects (axonal elongation) and the development of functional skeletal muscle tissue (myoblast fusion) are examples of physiological processes requiring intimate cell-cell interaction. Strategies to bridge nerve gaps using a variety of natural and synthetic scaffolding materials have been only moderately successful even in gaps less than 10 mm in length,^{18,19} and reasons for failure in many cases include lack of adequate pore interconnectivity and inadequate mechanical integrity of the conduit. Recent studies using porous poly(lactic-co-glycolic acid)²⁰ and poly(L-lactic acid)²¹ scaffolds for neural regeneration have shown promise in 12-mm nerve defects in a rat sciatic nerve model. Extension of this basic concept to larger, critical nerve defects may require controlled pore interconnectivity to allow vascular ingrowth, avoid pruning of regenerating fibers during axonal elongation and ensure that elongating axons reach their target organs. Several natural and synthetic scaffolds have also been proposed for regeneration of muscle tissue,²²⁻²⁴ and the major challenge in muscle regeneration may be promotion of aligned myoblast fusion within a three-dimensional scaffold construct to encourage formation of functional muscle tissue with adequate contractile properties.²⁵ Investigators have employed various cell seeding and tissue cultivation methods to promote cell-cell contact with some success.²⁶ Enhanced and controlled pore interconnectivity may be another attractive scaffold characteristic to advocate myoblast fusion. Further, the survival of cells within a functioning muscle organoid is diffusion limited,²⁷ and thus ingrowth of vascular tissue is essential to increase the maximum diameter of functional muscle constructs in order to amplify contractile properties. The salt fusion process may be particularly beneficial in preparing highly interconnected scaffolds for neural and muscular applications due to the substantial advantages of pore interconnectivity in promoting three-dimensional cell-cell interaction.

ACKNOWLEDGMENTS

We are grateful for financial support from the NIH (R01-DE-13349). We also would like to acknowledge the NIH for a cellular biotechnology training grant (T32 GM 08353) to W.L.M.

REFERENCES

1. Hutmacher, D.W. Scaffolds in tissue engineering bone and cartilage. *Biomaterials* **21**, 2529, 2000.
2. Chaignaud, B.E., Langer, R., and Vacanti, J.P. The history of tissue engineering using synthetic biodegradable polymer scaffolds and cells. In: A. Atala, and D.J. Mooney, eds. *Synthetic Biodegradable Polymer Scaffolds*. Boston: Birkhauser, 1997, pp. 1-14.
3. Murphy, W.L., and Mooney, D.J. Controlled delivery of inductive proteins, plasmid DNA and cells from tissue engineering matrices. *J. Periodontal Res.* **34**, 413, 1999.
4. Lu, L.C., and Mikos, A.G. The importance of new processing techniques in tissue engineering. *MRS Bull.* **21**, 28, 1996.

5. Mikos, A.G., Thorsen, A.J., Szerwonka, L.A., et al. Preparation and characterization of poly(L-lactic acid) foams. *Polymer* **35**, 1068, 1994.
6. Harris, L.D., Kim, B.S., and Mooney, D.J. Open pore biodegradable matrices formed with gas foaming. *J. Biomed. Mater. Res.* **42**, 396, 1998.
7. Kaufmann, P.M., Heimrath, S., Kim, B.S., et al. Highly porous polymer matrices as a three-dimensional culture system for hepatocytes. *Cell Transplant.* **6**, 463, 1997.
8. Oberpenning, F., Meng, J., Yoo, J.J., et al. *De novo* reconstitution of a functional mammalian urinary bladder by tissue engineering. *Nat. Biotechnol.* **7**, 149, 1999.
9. Freed, L.E., Marquis, J.C., Nohria, A., et al. Neocartilage formation *in vitro* and *in vivo* using cells cultured on synthetic biodegradable polymers. *J. Biomed. Mater. Res.* **27**, 11, 1993.
10. Ishaug-Riley, S.L., Crane, G.M., Gurlek, A., et al. Ectopic bone formation by marrow stromal osteoblast transplantation using poly(DL-lactic-co-glycolic acid) foams implanted into the rat mesentery. *J. Biomed. Mater. Res.* **36**, 1, 1997.
11. Kim, B.S., and Mooney, D.J. Engineering smooth muscle tissue with a predefined structure. *J. Biomed. Mater. Res.* **41**, 322, 1998.
12. Murphy, W.L., Kohn, D.H., and Mooney, D.J. Growth of continuous bone-like mineral within porous poly(lactide-co-glycolide) scaffolds *in vitro*. *J. Biomed. Mater. Res.* **50**, 50, 2000.
13. Ma, P.X., and Choi, J. Biodegradable polymer scaffolds with well-defined interconnected spherical pore network. *Tissue Eng.* **7**, 23, 2001.
14. Sheridan, M., Shea, L.D., Peters, M.C., et al. Bioabsorbable polymer scaffolds for tissue engineering capable of sustained growth factor delivery. *J. Control. Release* **64**, 91, 2000.
15. Murphy, W.L., Peters, M.C., Kohn, D.H., et al. Sustained release of vascular endothelial growth factor from mineralized poly(lactide-co-glycolide) scaffolds for tissue engineering. *Biomaterials* **21**, 2521, 2000.
16. Shea, L.D., Smiley, E., Bonadio, J., et al. DNA delivery from polymer matrices for tissue engineering. *Nat. Biotechnol.* **17**, 551, 1999.
17. Van Vlack, L. H. *Elements of Materials Science and Engineering*, 4th ed. Reading, MA: Addison-Wesley, 1980.
18. Valentini, R.F., Aebischer, P., Winn, S.R., et al. Collagen- and laminin-containing gels impede peripheral nerve regeneration through semipermeable nerve guidance channels. *Exp. Neurol.* **98**, 350, 1987.
19. Aldini, N.N., Perego, G., Cella, G.D., et al. Effectiveness of a bioabsorbable conduit in the repair of peripheral nerves. *Biomaterials* **17**, 959, 1996.
20. Evans, G.R.D., Brandt, K., Widmer, M.S., et al. Tissue engineered conduits: the use of biodegradable poly(D,L-lactic-co-glycolic acid) scaffolds in peripheral nerve regeneration. In: G.E. Stark, R. Horch, and E. Tanczos, eds. *Biological Matrices and Tissue Reconstruction*. Berlin: Springer, 1998, pp. 225–235.
21. Evans, G.R.D., Brandt, K., Widmer, M.S., et al. *In vivo* evaluation of poly(L-lactic acid) porous conduits for peripheral nerve regeneration. *Biomaterials* **20**, 1109, 1999.
22. van Wachem, P.B., Brouwer, L.A., and van Luyn, M.J.A. Absence of muscle regeneration after implantation of a collagen matrix seeded with myoblasts. *Biomaterials* **20**, 419, 1999.
23. Shansky, J., Chromiak, J., Del Tatto, M., et al. A simplified method for tissue engineering skeletal muscle organoids *in vitro*. *In Vitro Cell. Dev. Biol. Anim.* **33**, 659, 1997.
24. Okano, T., and Matsuda, T. Muscular tissue engineering: capillary-incorporated hybrid muscular tissues *in vivo* tissue culture. *Cell Transplant.* **7**, 435, 1998.
25. Swadison, S., and Mayne, R. Formation of highly organized skeletal muscle fibers *in vitro*: comparison with muscle development *in vivo*. *J. Cell. Sci.* **102**, 643, 1992.
26. Carrier, R.L., Papadaki, M., Rupnick, M., et al. *Biotech. Bioeng.* **64**, 580, 1999.
27. Dennis, R.G., and Kosnik, P.E. Excitability and isometric contractile properties of mammalian skeletal muscle constructs engineered *in vitro*. *In Vitro Cell. Dev. Biol. Anim.* **36**, 327, 2000.

Address reprint requests to:

David J. Mooney, Ph.D.

Departments of Chemical Engineering,

Biomedical Engineering, and Biologic

and Materials Sciences

University of Michigan

3074 H.H. Dow Building

2300 Hayward St.

Ann Arbor, MI 48109-2136

E-mail: mooneyd@engin.umich.edu

This article has been cited by:

1. Ville V. Meretoja, Minna Malin, Jukka V. Seppälä, Timo O. Närhi. 2009. Osteoblast response to continuous phase macroporous scaffolds under static and dynamic culture conditions. *Journal of Biomedical Materials Research Part A* **89A**:2, 317-325. [[CrossRef](#)]
2. Stéphanie Grenier, Martin Sandig, David W. Holdsworth, Kibret Mequanint. 2009. Interactions of coronary artery smooth muscle cells with 3D porous polyurethane scaffolds. *Journal of Biomedical Materials Research Part A* **89A**:2, 293-303. [[CrossRef](#)]
3. R. G. J. C. Heijkants, R. V. van Calck, T. G. van Tienen, J. H. de Groot, A. J. Pennings, P. Buma, R. P. H. Veth, A. J. Schouten. 2009. Polyurethane scaffold formation via a combination of salt leaching and thermally induced phase separation. *Journal of Biomedical Materials Research Part A* **87A**:4, 921-932. [[CrossRef](#)]
4. A. Martins, R. L. Reis, N. M. Neves. 2008. Electrospinning: processing technique for tissue engineering scaffolding. *International Materials Reviews* **53**:5, 257-274. [[CrossRef](#)]
5. H.-J. Wang, S.-J. Gong, J.-Y. Wang. 2008. Mechanical improvement of zein protein as scaffold for bone tissue engineering. *Materials Science and Technology* **24**:9, 1045-1052. [[CrossRef](#)]
6. Peter M. Crapo, Jin Gao, Yadong Wang. 2008. Seamless tubular poly(glycerol sebacate) scaffolds: High-yield fabrication and potential applications. *Journal of Biomedical Materials Research Part A* **86A**:2, 354-363. [[CrossRef](#)]
7. Cédryck Vaquette, Céline Frochot, Rachid Rahouadj, Xiong Wang. 2008. An innovative method to obtain porous PLLA scaffolds with highly spherical and interconnected pores. *Journal of Biomedical Materials Research Part B: Applied Biomaterials* **86B**:1, 9-17. [[CrossRef](#)]
8. Choll W. Kim, Robert Talac, Lichun Lu, Michael J. Moore, Bradford L. Currier, Michael J. Yaszemski. 2008. Characterization of porous injectable poly-(propylene fumarate)-based bone graft substitute. *Journal of Biomedical Materials Research Part A* **85A**:4, 1114-1119. [[CrossRef](#)]
9. Rouwayda El-Ayoubi , Nicoletta Eliopoulos , Robert Diraddo , Jacques Galipeau , Azizeh-Mitra Yousefi . 2008. Design and Fabrication of 3D Porous Scaffolds to Facilitate Cell-Based Gene Therapy. *Tissue Engineering Part A* **14**:6, 1037-1048. [[Abstract](#)] [[PDF](#)] [[PDF Plus](#)]
10. Rouwayda El-Ayoubi, Nicoletta Eliopoulos, Robert Diraddo, Jacques Galipeau, Azizeh-Mitra Yousefi. 2008. Design and Fabrication of 3D Porous Scaffolds to Facilitate Cell-Based Gene Therapy. *Tissue Engineering Part A*, ahead of print080422095744451. [[CrossRef](#)]
11. Ronny Pini, Giuseppe Storti, Marco Mazzotti, Hongyun Tai, Kevin M. Shakesheff, Steven M. Howdle. 2008. Sorption and swelling of poly(DL-lactic acid) and poly(lactic-co-glycolic acid) in supercritical CO₂: An experimental and modeling study. *Journal of Polymer Science Part B: Polymer Physics* **46**:5, 483-496. [[CrossRef](#)]
12. Michael Shin, Harutsugi Abukawa, Maria J. Troulis, Joseph P. Vacanti. 2008. Development of a biodegradable scaffold with interconnected pores by heat fusion and its application to bone tissue engineering. *Journal of Biomedical Materials Research Part A* **84A**:3, 702-709. [[CrossRef](#)]
13. Jungwoo Lee , Meghan J. Cuddihy , Nicholas A. Kotov . 2008. Three-Dimensional Cell Culture Matrices: State of the Art. *Tissue Engineering Part B: Reviews* **14**:1, 61-86. [[Abstract](#)] [[PDF](#)] [[PDF Plus](#)]
14. Mieke Heyde, Kris A. Partridge, Steven M. Howdle, Richard O.C. Oreffo, Martin C. Garnett, Kevin M. Shakesheff. 2007. Development of a slow non-viral DNA release system from PDLA scaffolds fabricated using a supercritical CO₂ technique. *Biotechnology and Bioengineering* **98**:3, 679-693. [[CrossRef](#)]

15. Stéphanie Grenier, Martin Sandig, Kibret Mequanint. 2007. Polyurethane biomaterials for fabricating 3D porous scaffolds and supporting vascular cells. *Journal of Biomedical Materials Research Part A* **82A**:4, 802-809. [[CrossRef](#)]
16. Feng Xu, Karen J. L. Burg. 2007. Three-dimensional polymeric systems for cancer cell studies. *Cytotechnology* **54**:3, 135-143. [[CrossRef](#)]
17. Er Liu, Matthew D. Treiser, Patrick A. Johnson, Parth Patel, Aarti Rege, Joachim Kohn, Prabhas V. Moghe. 2007. Quantitative biorelevant profiling of material microstructure within 3D porous scaffolds via multiphoton fluorescence microscopy. *Journal of Biomedical Materials Research Part B: Applied Biomaterials* **82B**:2, 284-297. [[CrossRef](#)]
18. Mark J. Butler, Michael V. Sefton. 2007. Poly(butyl methacrylate-co-methacrylic acid) tissue engineering scaffold with pro-angiogenic potential in vivo. *Journal of Biomedical Materials Research Part A* **82A**:2, 265-273. [[CrossRef](#)]
19. J. F. Mano, R. L. Reis. 2007. Osteochondral defects: present situation and tissue engineering approaches. *Journal of Tissue Engineering and Regenerative Medicine* **1**:4, 261-273. [[CrossRef](#)]
20. Qiang Fu, Mohamed N. Rahaman, B. Sonny Bal, Wenhai Huang, Delbert E. Day. 2007. Preparation and bioactive characteristics of a porous 13–93 glass, and fabrication into the articulating surface of a proximal tibia. *Journal of Biomedical Materials Research Part A* **82A**:1, 222-229. [[CrossRef](#)]
21. Hui Liu, Dharmaraj Raghavan, John Stubbs. 2007. Evaluation of the biological responses of osteoblast-like UMR-106 cells to the engineered porous PHBV matrix. *Journal of Biomedical Materials Research Part A* **81A**:3, 669-677. [[CrossRef](#)]
22. Daniel A. Shimko, Eric A. Nauman. 2007. Development and characterization of a porous poly(methyl methacrylate) scaffold with controllable modulus and permeability. *Journal of Biomedical Materials Research Part B: Applied Biomaterials* **80B**:2, 360-369. [[CrossRef](#)]
23. A. Sannino, P. A. Netti, M. Madaghiele, V. Coccoli, A. Luciani, A. Maffezzoli, L. Nicolais. 2006. Synthesis and characterization of macroporous poly(ethylene glycol)-based hydrogels for tissue engineering application. *Journal of Biomedical Materials Research Part A* **79A**:2, 229-236. [[CrossRef](#)]
24. Leenaporn Jongpaiboonkit, John W. Halloran, Scott J. Hollister. 2006. Internal Structure Evaluation of Three-Dimensional Calcium Phosphate Bone Scaffolds: A Micro-Computed Tomographic Study. *Journal of the American Ceramic Society* **89**:10, 3176-3181. [[CrossRef](#)]
25. Herman Blomeier, Xiaomin Zhang, Christopher Rives, Marcela Brissova, Elizabeth Hughes, Marshall Baker, Alvin C. Powers, Dixon B. Kaufman, Lonnie D. Shea, William L. Lowe. 2006. Polymer Scaffolds as Synthetic Microenvironments for Extrahepatic Islet Transplantation. *Transplantation* **82**:4, 452-459. [[CrossRef](#)]
26. V.V. Meretoja, A.O. Helminen, J.J. Korventausta, V. Haapa-aho, J.V. Seppälä, T.O. Närhi. 2006. Crosslinked poly(ϵ -caprolactone/D,L-lactide)/bioactive glass composite scaffolds for bone tissue engineering. *Journal of Biomedical Materials Research Part A* **77A**:2, 261-268. [[CrossRef](#)]
27. Manuela E. Gomes , Heidi L. Holtorf , Rui L. Reis , Antonios G. Mikos . 2006. Influence of the Porosity of Starch-Based Fiber Mesh Scaffolds on the Proliferation and Osteogenic Differentiation of Bone Marrow Stromal Cells Cultured in a Flow Perfusion Bioreactor. *Tissue Engineering* **12**:4, 801-809. [[Abstract](#)] [[PDF](#)] [[PDF Plus](#)]
28. Jin Gao , Peter M. Crapo , Yadong Wang . 2006. Macroporous Elastomeric Scaffolds with Extensive Micropores for Soft Tissue Engineering. *Macroporous Elastomeric Scaffolds with*

Extensive Micropores for Soft Tissue Engineering. *Tissue Engineering* **12**:4, 917-925. [[Abstract](#)] [[PDF](#)] [[PDF Plus](#)]

29. Junchuan Zhang, Hong Zhang, Linbo Wu, Jiandong Ding. 2006. Fabrication of three dimensional polymeric scaffolds with spherical pores. *Journal of Materials Science* **41**:6, 1725-1731. [[CrossRef](#)]
30. C. J. Bettinger, E. J. Weinberg, K. M. Kulig, J. P. Vacanti, Y. Wang, J. T. Borenstein, R. Langer. 2006. Three-Dimensional Microfluidic Tissue-Engineering Scaffolds Using a Flexible Biodegradable Polymer. *Advanced Materials* **18**:2, 165-169. [[CrossRef](#)]
31. L. Draghi, S. Resta, M. G. Pirozzolo, M. C. Tanzi. 2006. Microspheres leaching for scaffold porosity control. *Journal of Materials Science: Materials in Medicine* **16**:12, 1093-1097. [[CrossRef](#)]
32. Scott J. Hollister. 2005. Porous scaffold design for tissue engineering. *Nature Materials* **4**:7, 518-524. [[CrossRef](#)]
33. A. N. Stachowiak, A. Bershteyn, E. Tzatzalos, D. J. Irvine. 2005. Bioactive Hydrogels with an Ordered Cellular Structure Combine Interconnected Macroporosity and Robust Mechanical Properties. *Advanced Materials* **17**:4, 399-403. [[CrossRef](#)]
34. U. Kneser, A. Voogd, J. Ohnolz, O. Buettner, L. Stangenberg, Y.H. Zhang, G.B. Stark, D.J. Schaefer. 2005. Fibrin Gel-Immobilized Primary Osteoblasts in Calcium Phosphate Bone Cement: In vivo Evaluation with Regard to Application as Injectable Biological Bone Substitute. *Cells Tissues Organs* **179**:4, 158-169. [[CrossRef](#)]
35. A.L. Darling, Wei Sun. 2005. Free-form fabrication and micro-CT characterization of poly-/spl epsiv/-caprolactone tissue scaffolds. *IEEE Engineering in Medicine and Biology Magazine* **24**:1, 78-83. [[CrossRef](#)]
36. Jung Yul Lim , Amanda F. Taylor , Zhongyong Li , Erwin A. Vogler , Henry J. Donahue . 2005. Integrin Expression and Osteopontin Regulation in Human Fetal Osteoblastic Cells Mediated by Substratum Surface Characteristics. *Tissue Engineering* **11**:1-2, 19-29. [[Abstract](#)] [[PDF](#)] [[PDF Plus](#)]
37. Young Shin Kim , Jung Yul Lim , Henry J. Donahue , Tao Lu Lowe . 2005. Thermoresponsive Terpolymeric Films Applicable for Osteoblastic Cell Growth and Noninvasive Cell Sheet Harvesting. *Tissue Engineering* **11**:1-2, 30-40. [[Abstract](#)] [[PDF](#)] [[PDF Plus](#)]
38. Limin Guan, John E. Davies. 2005. Preparation and characterization of a highly macroporous biodegradable composite tissue engineering scaffold. *Journal of Biomedical Materials Research* **71A**:3, 480-487. [[CrossRef](#)]
39. Tejas S. Karande, Joo L. Ong, C. Mauli Agrawal. 2005. Diffusion in Musculoskeletal Tissue Engineering Scaffolds: Design Issues Related to Porosity, Permeability, Architecture, and Nutrient Mixing. *Annals of Biomedical Engineering* **32**:12, 1728-1743. [[CrossRef](#)]
40. K. R. King, C. C. J. Wang, M. R. Kaazempur-Mofrad, J. P. Vacanti, J. T. Borenstein. 2004. Biodegradable Microfluidics. *Advanced Materials* **16**:22, 2007-2012. [[CrossRef](#)]
41. Michael J. Moore, Esmail Jabbari, Erik L. Ritman, Lichun Lu, Bradford L. Currier, Anthony J. Windebank, Michael J. Yaszemski. 2004. Quantitative analysis of interconnectivity of porous biodegradable scaffolds with micro-computed tomography. *Journal of Biomedical Materials Research* **71A**:2, 258-267. [[CrossRef](#)]

42. A. L. Darling, W. Sun. 2004. 3D microtomographic characterization of precision extruded poly- ϵ -caprolactone scaffolds. *Journal of Biomedical Materials Research* **70B**:2, 311-317. [[CrossRef](#)]
43. Orasa Anusaksathien, Qiming Jin, Ming Zhao, Martha J. Somerman, William V. Giannobile. 2004. Effect of Sustained Gene Delivery of Platelet-Derived Growth Factor or Its Antagonist (PDGF-1308) on Tissue-Engineered Cementum. *Journal of Periodontology* **75**:3, 429-440. [[CrossRef](#)]
44. Qingpu Hou, Dirk W. Grijpma, Jan Feijen. 2003. Preparation of interconnected highly porous polymeric structures by a replication and freeze-drying process. *Journal of Biomedical Materials Research* **67B**:2, 732-740. [[CrossRef](#)]
45. Q.-M. Jin, M. Zhao, S.A. Webb, J.E. Berry, M.J. Somerman, W.V. Giannobile. 2003. Cementum engineering with three-dimensional polymer scaffolds. *Journal of Biomedical Materials Research* **67A**:1, 54-60. [[CrossRef](#)]
46. Hilary Tovey. 2003. Theorising Nature and Society in Sociology: The Invisibility of Animals. *Sociologia Ruralis* **43**:3, 196-215. [[CrossRef](#)]
47. Raymond Murphy. 2002. The internalization of autonomous nature into society¹. *The Sociological Review* **50**:3, 314-333. [[CrossRef](#)]